

Bouncing compact objects II: Effective theory of a pulsating Planck star

Jibril Ben Achour,^{a,1} Jean-Philippe Uzan^b

^aYukawa Institute for Theoretical Physics, Kyoto University, 606-85502, Kyoto, Japan

^bInstitut d'Astrophysique de Paris, CNRS UMR 7095, Université Pierre et Marie Curie - Paris VI, 98 bis Boulevard Arago, 75014 Paris, France

E-mail: jibril.benachour@yukawa.kyoto-u.ac.jp, uzan@iap.fr

Abstract. This article presents an effective quantum extension of the seminal Oppenheimer-Snyder (OS) collapse in which the singularity resolution is modeled using the effective dynamics of the spatially closed loop quantum cosmology. Using the Israel-Darmois junction conditions, it shows that one can consistently glue this bouncing LQC geometry to the classical vacuum exterior Schwarzschild geometry across a time-like thin-shell. Consistency of the construction leads to several major deviations from the classical OS collapse model. Firstly, no trapped region can form and the bounce occurs always above, or at most at the Schwarzschild radius. Secondly, the bouncing star discussed here admits an IR cut-off, additionally to the UV cut-off and corresponds therefore to a pulsating compact object. Thirdly, the scale at which quantum gravity effects become non-negligible is encoded in the ratio between the UV cut-off of the quantum theory and the IR cut-off, which in turn, encodes the minimal energy density ρ_{\min} of the star prior to collapse. This energy density is no more fixed by the mass and maximal radius as in the classical OS model, but is now a free parameter of the model. In the end, while the present model cannot describe a black-to-white hole bounce as initially suggested by the Planck star model, it provides a concrete realization of a pulsating compact object based on LQC techniques. Consistency of the model shows that its regime of applicability is restricted to planckian relics while macroscopic stellar objects are excluded. This first minimal construction should serve as a platform for further investigations in order to explore the physics of bouncing compact objects within the framework of loop quantum cosmology.

¹Corresponding author.

Contents

1	Introduction	2
2	Summary of the model	4
2.1	Interior solution	4
2.1.1	Spacetime geometry	5
2.1.2	Generic interior dynamics	5
2.2	Exterior solution	6
2.3	Junction conditions with a surrounding thin shell	7
2.4	Extended mass relation	8
2.5	Properties of the thin shell	9
2.5.1	Surface energy density	9
2.5.2	Surface pressure	9
2.6	Absence of trapped regions	10
2.7	Summary	10
3	UV completion from Loop Quantum Cosmology	11
3.1	Connection regularization - overview	11
3.2	Evolution of the quantum correction Ψ_1	12
3.3	Dynamics of the oscillating closed universe (interior region)	14
3.3.1	Reduced form of the dynamical equations	14
3.3.2	Minimal radius	15
3.3.3	Cycles of bounces	17
3.3.4	Cosmological implications	17
4	Modeling a pulsating Planck star	18
4.1	Properties of the thin shell	18
4.2	Quantum vs classical collapse	20
4.2.1	The classical Oppenheimer-Snyder model with a thin shell	20
4.2.2	Comparison of the dynamics and classical limit	21
4.3	Phase diagram of the Planck star	22
4.4	Orders of magnitude	23
5	Conclusion	25

1 Introduction

The existence of ultra compact objects is now routinely confirmed by the newly born gravitational waves astronomy. While black hole solutions of General Relativity (GR) provide to date the best model to fit the associated data, the existence of singularities in their core prevent them from providing a complete and self consistent UV description for these ultra compact objects. The resolution of these classical singularities can be addressed only within a quantum theory of gravity, in which the fate of the quantum geometry at high energy can be answered non perturbatively. As it turns out, the consequence of singularity resolution might be especially relevant from an observational point of view. Indeed, it is worth keeping in mind that these astronomical ultra compact objects being certainly not described by the stationary solutions of GR all the way down to the Planck scale, the absence of singularity in their core might have interesting observational effects. Since no complete quantum theory of gravity is yet available, the common strategy to capture the description of UV complete compact objects is to resort on effective approaches.

Over the last five years, important efforts have been devoted in investigating the consequences of singularity resolution within the classical gravitational collapse scenario. Among different proposals, the Planck star model presented in Ref. [1] has suggested new fascinating perspectives regarding the final stage of evaporating compact objects. Motivated by results in loop quantum cosmology, see e.g. Ref. [2] for a review, it was proposed that, after forming a trapping horizon, a collapsing star might form a planckian core, and subsequently bounces out due to the repulsive quantum gravity pressure, releasing the information store in the long-lived trapped region. Two crucial ideas were introduced to model this scenario. First, it was pointed that the energy scale at which quantum gravity effects become non-negligible *is not* dictated by the size of the object w.r.t to the Planck length, i.e. $\ell/\ell_{\text{Planck}}$, but by its density w.r.t the Planck density, i.e. $\rho/\rho_{\text{Planck}}$, allowing therefore quantum gravity to kick off at much above the Planck length. Moreover, it was suggested that while the bounce can be very short in the proper frame of the star, it appears extremely slow for an observer at infinity due to the huge gravitational time dilatation, allowing the model to be consistent with observational constraints. This elegant mechanism was applied to primordial black holes and phenomenological consequences were investigated in Refs. [3–7], suggesting a new observational window towards quantum gravity. More refined constructions of the dynamical geometry describing such bouncing compact object, and in particular the tunneling between the trapped to the anti-trapped region, were investigated later on, leading to the black hole firework and its further generalizations [8–12]. See also Refs. [13–15] for an alternative construction of a black-to-white hole tunnelling, based on a radically different mechanism. Finally, efforts to take into account the evaporation process were also discussed recently in Refs. [16–19]. See also Refs. [20–24] for recent investigations on the semi-classical description of evaporating and collapsing null shells.

This body of results suggests a new radically different scenario for the final stage of an evaporating and collapsing object which beg for further developments. In particular, can we construct a consistent model of a dynamical Planck star where the singularity resolution in the interior region is modeled by loop quantum cosmology technics? Important efforts have been devoted recently to implement such technics to discussed polymer interior black holes, which correspond to vacuum homogeneous geometries, see e.g. Refs. [33–48] and more recently Refs. [49, 50] for details¹. In order to develop a Planck star model, one needs to

¹See also Refs. [25–32] for earlier works on this topic.

go beyond this framework and consistently includes the role of collapsing matter. Previous attempts in this direction were presented in Refs. [51–58] as well as in Refs. [60–62] following a different approach. In this work, we adopt a different strategy. Using the quantum extension of the Oppenheimer-Snyder model presented in our companion article[65], we present a new construction, based on the thin shell formalism, which allows one to discuss matter collapse using LQC technics, and provides therefore a minimal set up to realize concretely, within the LQC framework, part of the ideas introduced in the initial Planck star model in Ref. [1].

To that goal, the interior homogenous geometry will be modeled by the loop quantum spatially closed cosmology filled with dust, discussed in Refs. [76, 77], while the exterior will be the classical Schwarzschild geometry. The singularity resolution, which manifests through a bounce at some critical energy, requires the existence of a non-vanishing energy-momentum localized on the thin shell joining the exterior and interior geometries. This time-like thin-shell plays a central role in that it encodes part of the quantum effects. In order to find admissible solutions for its surface energy and pressure, a key condition has to be satisfied, which arises from the generalization of the standard mass relation found by Oppenheimer and Snyder [78]. It ensures that the constants of motion associated to the exterior and interior geometries properly match during the whole process. Additionnaly, it translates into a constraint on the energy scale at which the bounce, and therefore the quantum gravity effects, becomes non-negligible.

In this regard, the present model allows one to implement the different ideas discussed earlier. It implements the singularity resolution mechanism using LQC technics, it includes the role of matter collapse which is modeled by a dust fluid, and it describes both the exterior and interior geometry of a UV complete bouncing compact object while ensuring the conservation laws during the whole process. As such, this simple model provides the minimal set up to discuss an effective UV complete gravitational collapse and its internal consistency using the technics of LQC. Let us emphasize the major outcomes of this construction.

Under the set of hypothesis discussed above, it was shown in Ref. [65] that such idealized bouncing object does not form a trapped region. The compact object forms at best a marginally trapping horizon, but automatically bounces at most at the energy threshold of horizon formation. As such, no black hole (as defined by the existence of a trapped region) is formed. This result provides a major deviation from the classical Oppenheimer-Snyder model where an event horizon and a subsequent singularity are formed as a result of the collapse. Moreover, it directly implies that quantum effects dominate at scale larger than or at the Schwarzschild radius, where the bounce occurs. As emphasized in Ref. [65], this is a direct consequence of demanding continuity of the induced metric across the time-like thin-shell, as well as working with a vacuum classical Schwarzschild exterior geometry. Hence, this no-go is intimately tied to these assumptions. Consequently, no long-lived trapped region can be described in this model, which suggests that additional structures are required to properly realize a model of Planck star as proposed in Ref. [1]. In particular, the lack of an inner horizon in the present model appears as the main missing ingredient.

Nevertheless, the present model provides a concrete framework to discuss the phenomenology of a UV complete pulsating star. Indeed, the interior geometry being modeled by a spatially closed bouncing universe, it enjoys both a UV and IR cut-offs denoted respectively $\tilde{\lambda}$ and R_c . As a result, the bouncing star follows cycles of expansion and contraction. This IR cut-off turns out to play a subtle role in this model. It encodes the minimal energy density ρ_{\min} of the star prior to collapse and contrary to the classical OS model where it is fixed by choosing the mass and maximal radius of the object, it is now a free parameter. Hence, com-

compact objects are now described in a parameter space with one additional dimension, which allows one to consider at fixed mass and radius new much denser compact objects. This is a major novelty of the present construction. Finally, the scale at which quantum gravity becomes non-negligible is encoded in the ratio $\tilde{\lambda}/R_c$. While the UV cut-off $\tilde{\lambda}$ is expected to be universal and fixed once and for all, it is nevertheless possible to shift this scale thanks to the free IR cut-off, i.e. by increasing the initial density ρ_{\min} . This provides a concrete realization of the Planck star idea where the scale associated to quantum gravity effects is encoded in the density of the compact object. Finally, we discuss the typical order of magnitude of the compact objects which can be described by our model, and show that they correspond to Planckian relics but not to standard macroscopic stellar objects.

To summarize, this work presents a minimal set up to implement the heuristic proposal of the Planck star using concrete techniques from LQC to account for the singularity resolution. Despite the no-go result discussed in Ref. [65], which prevents the present model to discuss black-to-white hole bounce, the present construction shall serve as a platform to investigate the phenomenology of this pulsating star and as a guideline for further developments. More realistic assumptions might be introduced to evade the no-go and describe long-lived trapped region, such as a non-vacuum exterior geometry with an outer and inner horizons structure as presented in Ref. [66] for example. Moreover, more refined corrections to describe the interior dynamics could be used, such as inverse triad corrections [79].

This article is organized as follows. Section 2 summarizes the effective construction developed in our companion article [65]. Then, Section 3 describes the UV completion that arises from loop quantum gravity, revisiting and extending the results of the existing literature, among which analytic formula for the minimal radius at the bounce. Then, Section 4 is devoted to the construction Planck star model. It presents the energy and pressure profiles of the thin shell, as well as its phase diagram, the dynamics of the star, its classical limit and the domain of applicability of our model.

2 Summary of the model

Let us start by summarizing the effective construction presented in our companion article [65], and recall briefly the generic constraint on the bouncing compact object. In this model, the star is described by an ideal ball of dust (i.e. zero pressure) of constant mass M , with a time-dependent energy density ρ , which undergoes a gravitational collapse. The full spacetime is then constructed by gluing a static exterior geometry with this time-dependent interior "cosmological" geometry. The gluing is performed on a time-like thin shell which corresponds to the surface of the star. The junction conditions, which encode the consistency of this gluing, impose the continuity of the induced metric, $[\gamma_{\alpha\beta}] = 0$ across the time-like thin shell while the jump of the extrinsic curvature defines the effective stress-energy tensor localized on the thin shell, $[K_{\alpha\beta} - \gamma_{\alpha\beta}K] = 8\pi G\sigma_{\alpha\beta}$. As we are going to see, the requirement of the continuity of the induced metric turns out to have far reaching consequences when assuming that the interior region is a regular bouncing geometry.

2.1 Interior solution

Following the OS model, we shall assume that the interior geometry corresponds to a closed Friedmann-Lemaître (FL) universe. However, the goal being to model a UV complete gravitational collapse, we shall introduce modified Friedman equations in which the effective

quantum corrections are parameterized in a general form. This will allow us to draw general conclusions independent of the specific form of the quantum corrections.

2.1.1 Spacetime geometry

Hence, the interior spacetime is assumed to have spatial sections that are homogeneous and isotropic with the topology of a 3-sphere. Therefore, its metric is of the (FL) form

$$ds_-^2 = -d\tau^2 + a^2(\tau)R_c^2 [d\chi^2 + \sin^2 \chi d\Omega^2] \quad (2.1)$$

where R_c is the constant curvature scale of the spatial sections. χ is the radial distance, in units of R_c , from the center and a the scale factor describing the homologous evolution of the star. τ is the proper time of free-falling observers at the surface of the sphere defined by

$$\Sigma : \chi = \chi_0. \quad (2.2)$$

By construction, the unit normal vector is radial, $n_\mu dx^\mu = a(\tau)d\chi$. These observers have a 4-velocity $u^\mu = (1, 0, 0, 0)$ so that $u_\mu dx^\mu = d\tau$. The outer radius of the star evolves as

$$R(\tau) = a(\tau)R_c \sin \chi_0 \quad (2.3)$$

and R_c has been chosen as units of length. Since the star shall have a radius smaller than the spatial section, it can always be written as $\sin \chi_0$ if initially we set $a_0 = 1$. The associated Hubble function is defined as

$$\mathcal{H} = \frac{a'}{a}, \quad (2.4)$$

with a prime referring to a derivative with respect to τ . Finally, the induced metric $\gamma_{\alpha\beta}^-$ and extrinsic curvature $K_{\alpha\beta}^-$ as seen from the interior region are given by

$$\gamma_{\mu\nu}^- dx^\mu dx^\nu = -d\tau^2 + a^2 R_c^2 \sin^2 \chi_0 d\Omega^2, \quad (2.5)$$

$$K_{\mu\nu}^- dx^\mu dx^\nu = R_c a \sin \chi_0 \cos \chi_0 d\Omega^2. \quad (2.6)$$

2.1.2 Generic interior dynamics

The dynamics of the interior region is assumed to follow some modified Friedmann equations to include the quantum corrections. In full generality, we assume that they take the form

$$\mathcal{H}^2 = \left(\frac{8\pi G}{3} \rho - \frac{1}{R_c^2 a^2} \right) [1 - \Psi_1(a)], \quad (2.7)$$

$$\mathcal{H}' = -4\pi G(\rho + P) [1 - \Psi_2(a)] + \frac{1}{R_c^2 a^2}, \quad (2.8)$$

where Ψ_1 and Ψ_2 are two functions that shall be specified by a choice of UV completion of GR. Furthermore, we assume the conservation of the matter stress-energy tensor, i.e.

$$\rho' = -3\mathcal{H}(\rho + P). \quad (2.9)$$

In the case of dust ($P = 0$), then

$$\rho = \mathcal{E} a^{-3} \quad (2.10)$$

with \mathcal{E} denoting the minimum of the energy density. Since at $\tau = 0$, $a_0 = 1$ and $a'_0 = 0$, one obtains

$$\mathcal{E} = \rho_{\min} = \frac{3}{8\pi G R_c^2}, \quad (2.11)$$

which corresponds to the minimum value, ρ_{\min} , of the matter energy density. Correspondingly, the maximal value of the physical radius is

$$R_{\max} = R_c \sin \chi_0. \quad (2.12)$$

This allows one to rewrite the modified Friedmann equations in the more compact form

$$\mathcal{H}^2 R_c^2 = \frac{1-a}{a^3} [1 - \Psi_1(a)], \quad (2.13)$$

$$R_c^2 \mathcal{H}' = \frac{1}{a^2} - \frac{3}{2} \frac{1}{a^3} [1 - \Psi_2(a)], \quad (2.14)$$

from which it follows, using Eq. (2.9), that

$$\Psi_2 = \left(1 - \frac{2}{3}a\right) \Psi_1(a) - \frac{a(1-a)}{3} \frac{d\Psi_1}{da}. \quad (2.15)$$

Finally, we note that the acceleration of the expansion is given by

$$\frac{a''}{a} R_c^2 = -\frac{1}{a^3} \left[\frac{1}{2} + \Psi_3(a) \right] \quad (2.16)$$

with

$$\Psi_3(a) = (1-a)\Psi_1(a) + \frac{3}{2}\Psi_2(a). \quad (2.17)$$

Note that so far we have kept the form of the effective quantum corrections unspecified. Hence, the interior of the star is modeled by a closed FL universe with a modified dynamics encoded by the function Ψ_1 . We can however draw some preliminary conclusions. If these corrections allow for a bounce, then there shall exist a time τ_b such that $\mathcal{H}(\tau_b) = 0$ and $\mathcal{H}'(\tau_b) > 0$. Generically, it implies that there shall exist a minimum value $a_{\min} \in]0, 1[$ such that $\Psi_1(a_{\min}) = 1$. Then, because of time reversibility and the absence of dissipation, this model will exhibit oscillatory solutions with $a \in]a_{\min}, 1]$ and the resulting compact object will have a characteristic pulsation depending solely on the parameters of the effective quantum theory.

2.2 Exterior solution

For simplicity, we assume that the exterior of the star is modeled by a classical spherically symmetric vacuum. Thanks to the Birkhoff's theorem, this selects the unique Schwarzschild solution to model the exterior geometry, such that the metric reads

$$ds_+^2 = -f(r)dt^2 + \frac{dr^2}{f(r)} + r^2 d\Omega^2 \quad (2.18)$$

with

$$f(r) = 1 - \frac{R_S}{r} \quad (2.19)$$

where R_S is the Schwarzschild radius

$$R_S \equiv 2GM. \quad (2.20)$$

As previously, we can always introduce χ_s such that

$$R_S = 2GM = R_c \sin \chi_s. \quad (2.21)$$

The induced metric of the hypersurface $\Sigma : r = r_*(t)$ describing the outer boundary of the star is given in Schwarzschild coordinates by

$$\gamma_{\mu\nu}^+ dx^\mu dx^\nu = -A^2[r_*(t)] dt^2 + r_*^2(t) d\Omega^2$$

where the function $A[r_*(t)]$ is related to the metric function $f(r)$ at $r = r_*(t)$ by demanding that the 4-velocity of the observer comoving with the sphere of symmetry remains a unit time-like vector, i.e $u^\alpha u_\alpha = -1$. This leads to

$$A[r_*(t)] = \sqrt{\frac{f^2[r_*(t)] - \dot{r}_*^2(t)}{f[r_*(t)]}}. \quad (2.22)$$

This expression of the lapse at the surface of the star, as seen by an exterior observer, shall play an important role in the following. The extrinsic curvature of Σ induced by the exterior Schwarzschild geometry reads in term of the (FL) coordinates system (τ, θ, ϕ)

$$K_{\mu\nu}^+ dx^\mu dx^\nu = -\frac{2A[r_*(t)]}{f[r_*(t)]} \left[\frac{d^2 r_*}{d\tau^2} + \frac{1}{2} f'[r_*(t)] \right] d\tau^2 + \frac{r_* f(r_*)}{A} d\Omega^2. \quad (2.23)$$

Notice that, assuming the exterior geometry is well-described by a vacuum spherically symmetric static solution of GR is indeed extremely constraining.

2.3 Junction conditions with a surrounding thin shell

In full generality the matching hypersurface can enjoy a non vanishing surface stress-energy tensor. As we will recall below, it vanishes in the original OS model [78]. However, in order to provide an effective quantum extension of this classical model, the presence of a thin-shell turns out to be crucial. Given the symmetries, the thin shell is well-described by a perfect fluid with surface energy density σ and pressure Π so that the surface stress-tensor $\sigma_{\alpha\beta}$ reads

$$\sigma_{\alpha\beta} = -\sigma u_\alpha u_\beta + \Pi (h_{\alpha\beta} + u_\alpha u_\beta). \quad (2.24)$$

Imposing the Israel-Darmois junction conditions, the continuity of the induced metric imposes that

$$r_*(t) = R_c a(\tau) \sin \chi_0 = R(\tau), \quad (2.25)$$

$$\frac{d\tau}{dt} = A(t), \quad (2.26)$$

from which it follows that

$$\dot{r}_*(t) = \frac{dr_*}{dt} = r_*(t) A[r_*(t)] \mathcal{H}(t). \quad (2.27)$$

The jump of the extrinsic curvature defines the surface stress-energy tensor components to be

$$\Sigma(t) = \frac{R_c}{r_*(t)} \left[\frac{f[r_*(t)]}{A[r_*(t)]} - \cos \chi_0 \right] \quad (2.28)$$

$$\bar{\Pi}(t) = -\frac{2R_c A^3[r_*(t)]}{f[r_*(t)]} \left[\frac{d^2 r_*}{d\tau^2} + \frac{1}{2} f'[r_*(t)] \right], \quad (2.29)$$

where we have introduced the dimensionless quantities

$$\Sigma \equiv 8\pi G R_c \sigma, \quad \bar{\Pi} \equiv 8\pi G R_c \Pi. \quad (2.30)$$

Notice that the second order derivative w.r.t. the radius r_* in the pressure expression is w.r.t. to the proper time τ .

Different routes can then be followed from that point. Either one has a specific micro-physical description of the shell that allows one to determine (Σ, Π) and then states whether the matching of these two geometries is doable. Or, one considers that the surface stress-tensor represents an effective way to take into account the modification of GR and that the matching conditions determine those properties. As explained in Ref. [65], we follow the second route. Let us finally point that the continuity of the induced metric does not depend on the properties of the shell.

2.4 Extended mass relation

The exterior and interior geometries involve two constants of motion M and \mathcal{E} . Upon solving the first junction condition for the extrinsic curvature (2.28), and using the relations (2.11-2.12) and (2.21) as well as Eq. (2.27), one obtains a dynamical relation relating these two constants of motion and the surface energy of the thin shell. This key relation is given by

$$M = \frac{4\pi}{3} \rho r_*^3 - \frac{r_*^3}{2GR_c^2} \left[\Sigma^2 + \frac{2R_c \cos \chi_0}{r_*} \Sigma + \frac{a-1}{a^3} \Psi_1 \right], \quad (2.31)$$

which can be recast into

$$\sin \chi_s = \sin^3 \chi_0 \left[1 - a^3 \left(\Sigma^2 + 2 \frac{\cot \chi_0}{a} \Sigma + \frac{a-1}{a^3} \Psi_1 \right) \right], \quad (2.32)$$

which depends explicitly on the effective quantum correction Ψ_1 . Let us discuss this matching constraint. First of all, in GR, i.e. when $\Psi_1 = 0$, the junction condition is possible without mass shell only if the standard OS condition is satisfied,

$$\sin \chi_s = \sin^3 \chi_0 \quad (2.33)$$

which just means that $M = 4\pi\rho(\tau)R^3(\tau)/3$. Hence, the standard mass relation obtained in the OS model is recovered if $\Psi_1 = 0$ and $\Sigma = 0$. It follows that otherwise (i.e. departure from GR or mismatch between the collapsing mass and exterior mass) the exterior and interior geometries can be glued only at the price of a shell. This extended mass relation turns out to play a key role in that it ensures that the conserved quantities associated to the exterior and interior geometries properly match during the whole evolution of the compact object, even during the bounce. A crucial outcome of this extended mass relation is that the energy of the dust \mathcal{E} , which is related to the IR cut-off, is now a free parameter of the model, contrary to the classical OS model where it is fixed by the mass M and the maximal radius $R_{\max} = R_c \sin \chi_0$. Hence, once the UV cut-off λ is fixed once and for all², the star is not parametrized by two but three independent parameters (R_c, χ_s, χ_0) . At fixed (χ_s, χ_0) , one has now the freedom to consider much denser objects.

²The Barbero-Immirzi parameter does not play any relevant role and can also be fixed to $\gamma = 1$ for simplicity

2.5 Properties of the thin shell

From the previous junction conditions have been obtained, we can now find suitable physical solution for the profile of the energy and pressure of the thin-shell.

2.5.1 Surface energy density

The relation (2.32) gives a second order polynomial equation for Σ ,

$$\Sigma^2 + 2\frac{\cot \chi_0}{a}\Sigma + \frac{1}{a^3} \left[\frac{\sin \chi_s}{\sin^3 \chi_0} - 1 - (a-1)\Psi_1 \right] = 0.$$

This sets a condition on the parameters of the star (χ_0, χ_s) and of the effective quantum theory through the dependency in Ψ_1 . Then, provided the reduced discriminant,

$$\Delta(a; \chi_0, \chi_s) = \frac{1}{a^2} \left\{ \cot^2 \chi_0 - \frac{1}{a} \left[\frac{\sin \chi_s}{\sin^3 \chi_0} - 1 + (1-a)\Psi_1 \right] \right\}, \quad (2.34)$$

is positive for all allowed values of a , the surface energy of the thin shell admits two solutions $\Sigma_{\pm}(a, \chi_0, \chi_s)$, given by

$$\Sigma_{\pm}(a; \chi_0, \chi_s) = -\frac{\cot \chi_0}{a} \pm \sqrt{\Delta(a; \chi_0, \chi_s)}. \quad (2.35)$$

Notice that, thanks to Eq. (2.28),

$$\frac{f[r_*(t)]}{A[r_*(t)]} = \pm a \sin \chi_0 \sqrt{\Delta(a; \chi_0, \chi_s)}. \quad (2.36)$$

Let us finally point that this solution to the junction condition has been obtained without specifying the quantum correction Ψ_1 .

2.5.2 Surface pressure

The expression of $\bar{\Pi}$ is obtained by disentangling the expression (2.29). Thanks to Eqs. (2.13-2.14), it reads

$$\bar{\Pi}(a; \chi_0, \chi_s) = -\frac{A_* \sin \chi_0}{f_* a^2} \left\{ \left(\frac{\sin \chi_s}{\sin^3 \chi_0} - 1 \right) + [3\Psi_2 - 2(1-a)\Psi_1] \right\}. \quad (2.37)$$

This expression completes the resolution of the junction conditions. We have therefore obtained a general resolution of the matching between our Schwarzschild exterior and the effective quantum closed universe. The profiles of the energy and pressure of the thin shell depend explicitly on the quantum correction Ψ_1 and its derivatives. Hence, the thin-shell can be understood as an effective way to encode part of the quantum effects for such a gluing. As a result, the quantum corrections will affect the thin-shell. If the surface of the collapsing compact object, crosses its Schwarzschild radius to form an event horizon, and if the quantum effects remain negligible at the horizon formation threshold and are triggered only near the would-be singularity, then, they could be considered as confined to the deep interior. However, as we are going to see now, consistency of the matching leads to a radically different picture, where the bounce turns out to occur prior to horizon formation, or at most, precisely at the horizon formation threshold.

2.6 Absence of trapped regions

One major question for such bouncing compact object is to which energy scale the quantum effects become dominant? Or in other word, at which energy scale the bounce occurs? It is widely believed that quantum gravity effects shall only be relevant in the deep interior region near the would be singularity.

As it turns out, a surprising outcome of our construction is to provide a constraint on the energy scale at which a bounce can occur. Let us summarize the main argument of Ref. [65]. First, notice that the expression of the lapse (2.22) can be recast in the more suggestive form

$$A^2[\tau] = \frac{f^2[r_*(\tau)]}{f[r_*(\tau)] + r_*^2(\tau)\mathcal{H}^2(\tau)} , \quad (2.38)$$

with

$$f[r_*(\tau)] = 1 - \frac{R_s}{r_*(\tau)} . \quad (2.39)$$

It is then straightforward to see that if a bounce occurs, i.e. if at some time τ_b , one has $\mathcal{H}(\tau_b) = 0$ and $\mathcal{H}'(\tau_b) > 0$, then the lapse at the bounce satisfies

$$A^2(\tau_b) = 1 - \frac{R_s}{r_*(\tau_b)} \geq 0. \quad (2.40)$$

For a star initially above the Schwarzschild radius, consistency imposes that $r_*(\tau) \geq R_s$ during the collapse and the bounce. This implies that the star never crosses its Schwarzschild radius such that it prevents a trapped region to form, and the time-like thin shell remains time-like at the bounce. To finish, note that while we are indeed working with a singular coordinate system at the horizon, the same computation can be done in the Eddington-Finkelstein coordinates, regular at the horizon, which leads to the very same result [65]. Notice also that this result is not contradictory with the bouncing black hole model built in Ref. [8], in which a collapsing null shell was considered. In that case, the key relation (2.38) responsible of our result is not present.

Finally, let us make one more remark. Assuming a bounce from quantum origin for the interior geometry, the above result might misleadingly suggests that quantum gravity effects are triggered at low curvature, which would go against the intuitive expectation. It turns out that this is not the case. In Section 4.4, we shall show that when the interior dynamics is modeled by a quantum bounce descending from loop quantum cosmology, consistency conditions severely restrict the range of applicability of the model. As it turns out, it can be shown that macroscopic stellar objects are excluded by this model, and only planckian relics can be consistently considered. For such extremely small mass and size objects, curvature is already very high even outside the horizon. As a consequence, even if the bounce occurs above or at the horizon scale, it still occurs in a regime of high curvature, as intuitively expected from a quantum bounce.

2.7 Summary

Without specifying the effective quantum corrections which ensure the UV completion of the interior dynamics, we have shown that one can still derive a general solution of the Israel-Darmois junction conditions, providing an effective theory for a UV complete gravitational collapse. The consistency of the model is encoded in the generalized mass relation (2.32). As a result, one obtains a general profile for the surface energy Σ and surface pressure Π of the

thin shell. Before discussing a concrete realization for the UV complete interior, let us recall the different assumptions of this construction. Following the thin shell approach developed in Ref. [65],

- the collapsing star is modeled as a closed FL universe with a modified UV complete dynamics. The UV completeness is encoded in the correction Ψ_1 which shall descend from the UV completion of GR. This implies that the dynamics of the scale factor can describe either a *bouncing star* or a *bouncing universe* and that it will remain independent, for the former, of the properties of the thin shell.
- The exterior of the star is the standard vacuum Schwarzschild geometry.
- The two geometries are glued on a time-like thin shell. Independently of the solution for the expansion $a(\tau)$, the properties of the thin shell are fully determined by the Israel-Darmois junction conditions. They depend on both the characteristic of the star (initial mass χ_s and initial radius χ_0) and on the function Ψ_1 which contains the parameters of the quantum theory. It follows that the physically acceptable solutions are constrained to satisfy the mass relation (2.32).

We have concluded that if Ψ_1 allows for a singularity resolution which manifests through a bounce of the star, then the compact object experiences cycles of contraction and expansion without black hole formation. This provides the basics of an effective theory of a pulsating Planck star. To go further one needs to choose Ψ_1 .

3 UV completion from Loop Quantum Cosmology

To be more specific, we now assume that Ψ_1 is determined by the corrections that arise in the loop regularization of the dynamics of spatially spherical universe presented in Refs. [74–77, 79]. Two different loop quantization schemes have been discussed in the literature, the so called curvature regularization [74, 75], and the connection regularization [76, 77], while additional refinement related to inverse volume corrections have been discussed in Ref. [79]. More recently, new phenomenology of this bouncing cosmology has been discussed in []. In what follows, we focus our attention on the connection regularization scheme, the curvature regularization scheme phenomenology will be discussed elsewhere.

3.1 Connection regularization - overview

Let us start by the modified Friedmann equations obtained in Ref. [76] and discuss their consequences for our model. While this model has already been investigated in Refs. [76, 77], the present section provides new analytic results regarding the expression of the minimal radius, as well as a clearer picture of the oscillating dynamics, and in particular the existence of two cycles of bounces associated to the two different minimal radii.

Consider the metric of a closed FL universe

$$ds^2 = -N^2 d\tau^2 + R_c^2 a^2(\tau) (d\chi^2 + \sin^2 \chi d\Omega^2). \quad (3.1)$$

Let us briefly summarize how the modified Friedmann equations are obtained within the LQC framework. Following the notations of Ref. [74], the gravitational canonical variables are given by

$$b \equiv \frac{c}{\sqrt{|p|}}, \quad v \equiv |p|^{3/2}, \quad \text{such that} \quad \{b, v\} = 4\pi G \gamma, \quad (3.2)$$

which correspond respectively to the Hubble factor and the 3-volume of the spatially closed universe. The dimension are given by $[b] = L^{-1}$, $[v] = L^3$. Then, using the loop regularization of the phase space of the closed FL universe [76], the modified dynamics is encoded in the polymer Hamiltonian constraint

$$\mathcal{S}_{\text{full}}[N] = N \left(v\rho - \frac{3}{8\pi G\gamma^2\tilde{\lambda}^2} v \left[(\sin \tilde{\lambda}b - D)^2 + \gamma^2 D^2 \right] \right) \simeq 0 \quad (3.3)$$

where ρ is the energy density, and we have introduced the short notation $D = \kappa/v^{1/3}$, hence related to the scale factor by

$$D(\tau) = \frac{\tilde{\lambda}}{R_c a(\tau)}. \quad (3.4)$$

It follows that the effective quantum theory depends on two parameters. The UV cut-off is encoded in the parameter $\tilde{\lambda}$, with dimension of length, i.e. $[\tilde{\lambda}] = L$, while γ is the Barbero-Immirzi parameter. without dimension. It is worth keeping in mind that these parameters are not fixed a priori, and shall be determined by experiments. The equations of motion w.r.t. the cosmic time τ , i.e. $N = 1$, are then given by

$$\dot{v} = \frac{3}{\gamma\tilde{\lambda}} v \left(\sin \tilde{\lambda}b - D \right) \cos \tilde{\lambda}b \quad (3.5)$$

$$\dot{b} = -\frac{3}{2\gamma\tilde{\lambda}^2} \left[\sin^2 \tilde{\lambda}b - \frac{4D}{3} \sin \tilde{\lambda}b + \frac{1}{3}(1 + \gamma^2)D^2 \right] \quad (3.6)$$

where we have assumed that $P = \partial_v(v\rho) = 0$, i.e. we work with a dust field of matter. The scalar constraint (3.3) can be recast as

$$\frac{\rho}{\rho_c} = (\sin \tilde{\lambda}b - D)^2 + \gamma^2 D^2, \quad (3.7)$$

where we have introduced the critical energy density

$$\rho_c \equiv \frac{3}{8\pi G\gamma^2\tilde{\lambda}^2} = \frac{\mathcal{E}}{\gamma^2(\tilde{\lambda}/R_c)^2}. \quad (3.8)$$

This concludes our description of the effective phase space and the associated effective dynamics of the closed FL geometry filled up with a perfect pressureless fluid.

3.2 Evolution of the quantum correction Ψ_1

From now on, we redefine the variables such that $\tau \rightarrow \tau/R_c$, and $b \rightarrow R_c b$. Rescaling also the UV cut-off the same way, we introduce the new dimensionless parameter

$$\lambda = \frac{\tilde{\lambda}}{R_c} \quad (3.9)$$

which shall play a crucial role in the following. Being the ratio of the UV and IR cut-offs, it encodes the scale at which quantum gravity effects become non-negligible. The interesting point is that the IR cut-off R_c is actually related to the energy density of the compact object prior to collapse, through the relation (2.11). Small value of R_c correspond to high. energy density. Now, while it is expected that the UV cut-off λ is an universal quantity fixed once and for all for any star, the parameter R_c is now a free parameter of the model which characterize

the star just as its mass and radius. Hence, by shifting the density of the compact object at fixed mass and radius, i.e at fixed (χ_s, χ_0) , one can now shift the effective scale of quantum gravity effects. This allows to implement the idea advocated in Ref. [1], that provided a compact object reaches a sufficiently large density w.r.t the Planck density, quantum gravity can be triggered even if the size of the object is much larger than the Planck length.

This implies that $D = \lambda/a$. Finally, one can introduce the rescaled Hubble factor and the rescaled critical energy

$$H = \mathcal{H}R_c, \quad \rho_c \equiv \frac{\mathcal{E}}{\gamma^2 \lambda^2}. \quad (3.10)$$

Since $v \propto a^3$, Eq. (3.5) implies that

$$H = \frac{1}{\gamma \lambda} (\sin \lambda b - D) \cos \lambda b. \quad (3.11)$$

This gives an expression for H^2 in which one can express $(\sin \lambda b - D)^2$ thanks to Eq. (3.7) as

$$(\sin \lambda b - D)^2 = \gamma^2 \lambda^2 \left(\frac{8\pi G}{3} \rho - \frac{1}{a^2} \right). \quad (3.12)$$

It follows from the definition (2.7) that $1 - \Psi_1 = \cos^2 \lambda b$, from which we conclude that

$$\Psi_1 = \sin^2 \lambda b. \quad (3.13)$$

This expression shows that $\Psi_1 = 1$ when $\lambda b = \pm\pi/2$. It follows that the first condition for the existence of a bounce is satisfied.

It can also be expressed in terms of a by using the expression for ρ and making use of Eq. (2.11) in Eq. (3.12) to express $\sin \lambda b$, leading to

$$\Psi_1 = \frac{\lambda^2}{a^2} \left(1 + \varepsilon \gamma \sqrt{\frac{1}{a} - 1} \right)^2 \quad (3.14)$$

where $\varepsilon = \pm 1$ is a sign that we shall discuss later. This expression allows us to get some insight on the dynamics. Fig. 1 shows the existence of two branches labeled by the sign of ε . If $\lambda < 1$, there will always exist two values,

$$0 < a_{\min}^{(-)} < a_{\min}^{(+)} < 1,$$

such that $\Psi_1(a) = 1$. By definition, $\Psi_1[a_{\min}^{(\pm)}] = 1$ corresponds to a vanishing Hubble factor, $H = 0$. Hence, we expect to have two different kinds of bounce. This was first pointed out in Ref. [76].

Following Ref.[76], it is useful to write down the modified Friedmann equations in the more familiar form

$$\mathcal{H}^2 = \frac{8\pi G}{3} \left(\rho - \frac{1}{R_c^2 a^2} \right) \left(1 - \frac{\rho - \rho_1}{\rho_c} \right) \quad (3.15)$$

$$\dot{\mathcal{H}} + \frac{1}{R_c^2 a^2} = -4\pi G \left(\rho - \frac{2\rho_1}{3} \right) \left(1 - \frac{\rho - \rho_2}{\rho_c} \right) \quad (3.16)$$

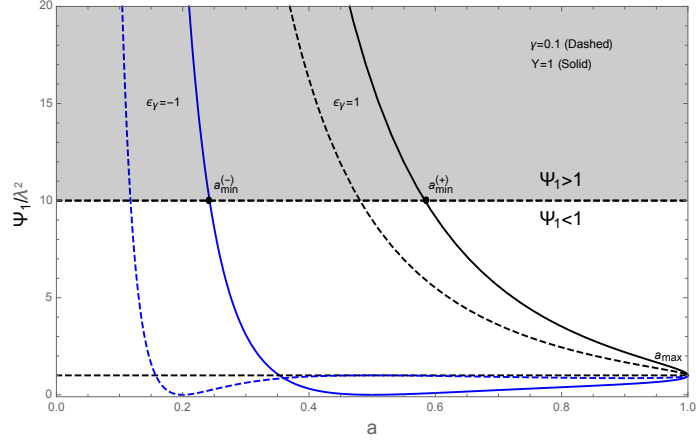


Figure 1. $\Psi_1(a)$ in units of λ^2 (black: $\varepsilon = +1$, blue: $\varepsilon = -1$) for $\gamma = 1$ (solid) and 0.1 (dashed). If $\lambda < 1$, there exists two values, $a_{\min}^{(-)} < a_{\min}^{(+)}$ for which $\Psi_1 = 1$, i.e. $H = 0$.

in terms of the densities

$$\rho_1 = \rho_c D [(1 + \gamma^2)D - 2 \sin(\lambda b)] \quad (3.17)$$

$$\rho_2 = \rho_c D [(1 + \gamma^2)D - \sin(\lambda b)] . \quad (3.18)$$

These forms allows us to extract the expressions of Ψ_1 and Ψ_2 in term of the density ρ and the critical densities ρ_1 and ρ_2 and ρ_c . Comparing with Eq. (2.7), one obtains

$$\Psi_1 = \frac{\rho - \rho_1}{\rho_c} \quad (3.19)$$

which can be checked to be equivalent to the expressions (3.13) and (3.14). To finish, Ψ_2 is obtained from Eq. (2.15). As a final remark, it is straightforward to check that the classical limit corresponds to

$$\lambda = \frac{\tilde{\lambda}}{R_c} \rightarrow 0 , \quad \Rightarrow \quad \rho_c \rightarrow +\infty , \quad D \rightarrow 0 , \quad \Psi_1 \rightarrow 0 \quad (3.20)$$

where we have used Eq. (3.17).

3.3 Dynamics of the oscillating closed universe (interior region)

As already discussed in Ref. [76], the bouncing dynamics encoded in the modified Friedmann equations (3.15-3.16) and (2.10) enjoys two bounces with two different allowed minimal radii. In order to understand the dynamics, it is useful to recast the equations of motion in a more suitable form. In the following, we provide the expression of the two allowed minimal radii and discuss the different cycles experienced by this bouncing closed universe.

3.3.1 Reduced form of the dynamical equations

It turns out to be convenient to introduce the variables

$$u \equiv 1/a, \quad X \equiv \sin \lambda b. \quad (3.21)$$

Concerning Eq. (3.5), one uses Eq. (3.12) with the expression (2.10) for the density to eliminate the quadratic term $\sin^2 \lambda b$ to finally get

$$\frac{du}{d\tau} = -\frac{u}{\lambda\gamma} \cos \lambda b (X - \lambda u) \quad (3.22)$$

$$\frac{dX}{d\tau} = -\lambda\gamma u \cos \lambda b \left\{ \frac{3}{2}u^2 - \frac{[(1 + \gamma^2)\lambda u - X]}{\lambda\gamma^2} \right\} \quad (3.23)$$

with

$$\cos \lambda b = \pm \sqrt{1 - X^2}. \quad (3.24)$$

This latter sign has no influence on the dynamics since it can be absorbed by the redefinition $\tau \rightarrow -\tau$. Additionally to this set of two equations of motion, the on shell system satisfies the constraint (3.12) that takes the form

$$(X - \lambda u)^2 = \gamma^2 \lambda^2 u^2 (u - 1), \quad (3.25)$$

which corresponds to satisfy the scalar constraint during the whole evolution.

3.3.2 Minimal radius

As seen from Fig. 1, we expect the dynamics to enjoy two minimal radii. Indeed the system (3.22-3.23) has 3 configurations in which $da/d\tau = 0$. The first one is obviously characterized by $u = 1$ (i.e. $a = 1$), which corresponds to the maximal extension of the star. It corresponds to the initial state which defines the initial conditions to integrate the system (3.22-3.23)

$$u = 1, \quad a = 1, \quad X = \lambda. \quad (3.26)$$

The second set of solutions is obtained for $\cos \lambda b = 0$, that is for

$$\lambda b = \frac{\pi}{2} + n\pi, \quad n \in \mathbb{Z}, \quad (3.27)$$

so that $\sin \lambda b = (-1)^n$. Inserting this condition in the effective Friedmann equation leads to

$$\lambda u [1 + \varepsilon\gamma\sqrt{u - 1}] = (-1)^n. \quad (3.28)$$

Since $u > 1$ (i.e. $a < 1$), we can define y such that $u = 1 + y^2$, so that the solutions of Eq. (3.28) are the roots $y_*(n, \lambda, \gamma)$ of

$$\lambda(y^2 + 1)(1 + \varepsilon\gamma y) = (-1)^n.$$

First, note that changing the sign of ε changes the sign of the root of this equation, which has no influence on the value of the physical variables u or a . So we can arbitrarily choose $\varepsilon = -1$. Then the solution with n odd and even are related by the change of the sign of λ . It follows that the solutions are $y_*(\lambda, \gamma)$ for $n = 2p$ and $y_*(-\lambda, \gamma)$ for $n = 2p + 1$ with y_* the root of

$$\lambda(y^2 + 1)(1 - \gamma y) = 1 \quad (3.29)$$

with $y > 0$. The determinant of this third order polynomial equation is given by

$$\Delta_O = 4\lambda^2 \left[(9\gamma^2 + 1) \lambda - \frac{27}{4}\gamma^2 - (1 + \gamma^2(2 + \gamma^2)) \lambda^2 \right]. \quad (3.30)$$

The nature of the roots (either complex or real) depends on the sign of Δ_O . In our case, the parameter γ is of order unity while $\lambda \ll 1$ for a realistic astrophysical object. Therefore, the first and last terms are very small compared to the middle term and one has therefore

$$\Delta_O \simeq -27\gamma^2\lambda^2 < 0. \quad (3.31)$$

This implies that the third order polynomial equation (3.29) has only one real root y_* supplemented with two complex conjugated roots that are therefore not physical. The only real root is

$$y_* = \frac{1}{3\gamma} \left[1 + \frac{2^{1/3}(3\gamma^2 - 1)}{\delta_2} - \frac{\delta_2}{2^{1/3}} \right] \quad (3.32)$$

with

$$\delta_2 = \left(-2 - 18\gamma^2 + 27\frac{\gamma^2}{\lambda} + \delta_1 \right)^{1/3}, \quad (3.33)$$

$$\delta_1 = \sqrt{4(3\gamma^2 - 1)^3 - \left(2 + 18\gamma^2 - 27\frac{\gamma^2}{\lambda} \right)}. \quad (3.34)$$

In conclusion, irrespective of the sign ε , the scale factor a enjoys two minima

$$a_{\min}^{(\pm)}(\gamma, \lambda) \equiv \frac{1}{y_*^2(\gamma, \pm\lambda) + 1}, \quad (3.35)$$

the sign of λ being related to the phase of λb that determines the sign of X . These minima satisfy $0 < a_{\min}^{(-)} < a_{\min}^{(+)} < 1$ and they scale as

$$a_{\min}^{(\pm)} \simeq \gamma^{2/3}\lambda^{2/3} \pm \frac{2}{3}\lambda \quad \text{as } \lambda \rightarrow 0. \quad (3.36)$$

Fig. 2 depicts the dependence of these minima with λ for different values of the parameter γ . As expected from Eq. (3.14), $a_{\min}^{(+)} \rightarrow 1$ when $\lambda \rightarrow 1$.

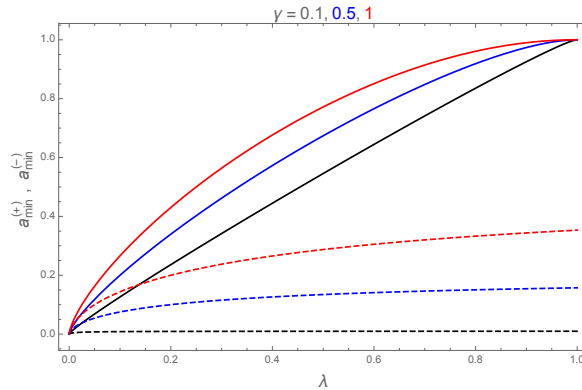


Figure 2. The evolution of $a_{\min}^{(+)}$ (solid) and $a_{\min}^{(-)}$ (dashed) with λ .

3.3.3 Cycles of bounces

The dynamics is completely described by Eqs. (3.22-3.23). As anticipated from the analysis of Fig. 1, it is clear that the system undergoes oscillations. Starting from the initial state ($a_0 = 1, X_0 = \lambda, dX/d\tau > 0$), it will reach the minimum and bounce. But when it reaches a_0 again, the sign of the derivative of X has been switched so that it starts another cycle with the same initial conditions but with $dX/d\tau < 0$. Hence, we have a succession of cycles with a period of 2 phases related to the $(-1)^n$ in Eq. (3.27), i.e.

$$\begin{pmatrix} a \\ X \end{pmatrix} : \begin{pmatrix} a_0 = 1 \\ X_0 = \lambda \end{pmatrix} \rightarrow \begin{pmatrix} a_{\min}^{(-)} \\ -1 \end{pmatrix} \rightarrow \begin{pmatrix} a_0 = 1 \\ X_0 = \lambda \end{pmatrix} \rightarrow \begin{pmatrix} a_{\min}^{(+)} \\ +1 \end{pmatrix} \rightarrow \begin{pmatrix} a_0 = 1 \\ X_0 = \lambda \end{pmatrix}. \quad (3.37)$$

The numerical integration of the system (3.22-3.23) is depicted on Fig. 3 and compared to the minimal radii (3.35). It confirms that there is an alternance of cycles related to the change of sign of X at the maximum expansion in $a = 1$. This tale of two bounces was first found numerically in Refs. [76, 77]. However, to our knowledge, the full analytical derivation of the two minima appears for the first time here, as well as the explanation for the shift between the two cycles.

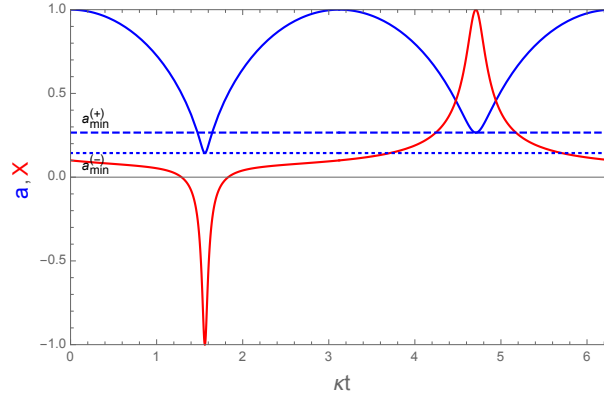


Figure 3. Evolution of a (blue) X (red). As expected from Eq. (3.37), the dynamics enjoys a cycle of two oscillations compared to $a_{\min}^{(+)}$ (dashed) and $a_{\min}^{(-)}$ (dotted). The two cycles are labeled by the sign of X , that is by ε .

3.3.4 Cosmological implications

The former description applies both to the dynamics of a collapsing star and to cosmology. It can be easily extended to consider matter with different equations of state, in particular to include a radiation fluid or a cosmological constant. We can rephrase the modifications of the Friedmann equations as the effects of an effective fluid with density ρ_Q and pressure P_Q that enter the standard Friedmann equations. It follows that

$$\rho_Q + P_Q = -(\rho + P)\Psi_2(a), \quad (3.38)$$

$$\frac{8\pi G}{3}\rho_Q = -\left(\frac{8\pi G}{3}\rho - \frac{1}{R_c^2 a^2}\right)\Psi_1(a). \quad (3.39)$$

These expressions show that generically the effect of the loop regularization is to induce the action of an effective fluid with negative pressure. The conservation equation $\rho' + 3\mathcal{H}(\rho + P) =$

0 gives the relation between Ψ_2 and Ψ_1 that generalizes Eq. (2.15) so that we end up with

$$\rho_Q = \left(-\rho + \frac{3}{8\pi G R_c^2 a^2} \right) \Psi_1(a) \quad (3.40)$$

$$\rho_Q + P_Q = - \left[(\rho + P) - \frac{1}{4\pi G R_c^2 a^2} \right] \Psi_1(a) + \left(\frac{1}{3}\rho - \frac{1}{8\pi G R_c^2 a^2} \right) a \frac{d\Psi_1}{da}. \quad (3.41)$$

Assuming that the standard matter enjoys a constant equation of state w , so that $\rho = \rho_0 a^{-3(1+w)}$, we get

$$\rho_Q = -\rho_0 \left(a^{-3(1+w)} - \frac{3}{8\pi G R_c^2 \rho_0 a^2} \right) \Psi_1(a) \quad (3.42)$$

$$\begin{aligned} \rho_Q + P_Q = & -\rho_0 \left[(1+w)a^{-3(1+w)} - \frac{2}{8\pi G R_c^2 \rho_0 a^2} \right] \Psi_1(a) \\ & -\rho_0 \left(-\frac{1}{3}a^{-3(1+w)} + \frac{1}{8\pi G R_c^2 \rho_0 a^2} \right) a \frac{d\Psi_1}{da}. \end{aligned} \quad (3.43)$$

Setting $\kappa_0 \equiv \frac{1}{8\pi G R_c^2 \rho_0}$ we get

$$\rho_Q = -\rho_0 \left(a^{-(1+3w)} - 3\kappa_0 \right) \frac{\Psi_1}{a^2} \quad (3.44)$$

$$P_Q = -\rho_0 \left[w a^{-(1+3w)} + \kappa_0 \right] \frac{\Psi_1}{a^2} - \rho_0 \left(-\frac{1}{3}a^{-(1+3w)} + \kappa_0 \right) \frac{1}{a} \frac{d\Psi_1}{da}. \quad (3.45)$$

These expressions can be used to determine the quantum corrections to the expansion history in a radiation universe or during inflation, a general phenomenological analysis that we postpone for now.

4 Modeling a pulsating Planck star

The dynamics of a bouncing homogeneous spacetime can be used to describe the interior of a collapsing star. We now turn to the construction of the Planck star model since the whole study of the UV-complete closed universe applies to the dynamics of the interior of such a star. What remains to be derived are indeed the physical properties of the thin shell, namely its energy and pressure profiles. Finally, one has to identify the sub-region of the parameters space for which the modelisation of the star is well-defined.

4.1 Properties of the thin shell

Let us first discuss the properties of the energy and pressure profiles. As in GR, there are two branches, one with $\Sigma = \Sigma_+ > 0$ and the other with $\Sigma = \Sigma_- < 0$, that we may consider as non-physical. The plot of the energy Σ of the thin shell is depicted in Fig. 4. As can be seen, the quantum corrections dominate when a reaches a_{\min} and vanishes on $a = 1$ so that we recover the GR shell properties, with a non vanishing surface energy density. As can also be seen, the total density of the shell, Σa^2 remains bounded and the quantum corrections dominate only close to the minimal radius, so that they induce the bounce. Similar conclusions for $\bar{\Pi}$ are presented on Fig. 5.

Therefore, the behavior of the energy and pressure profiles is consistent with the expectation that quantum effects are triggered near the bounce. However, since the bounce occurs

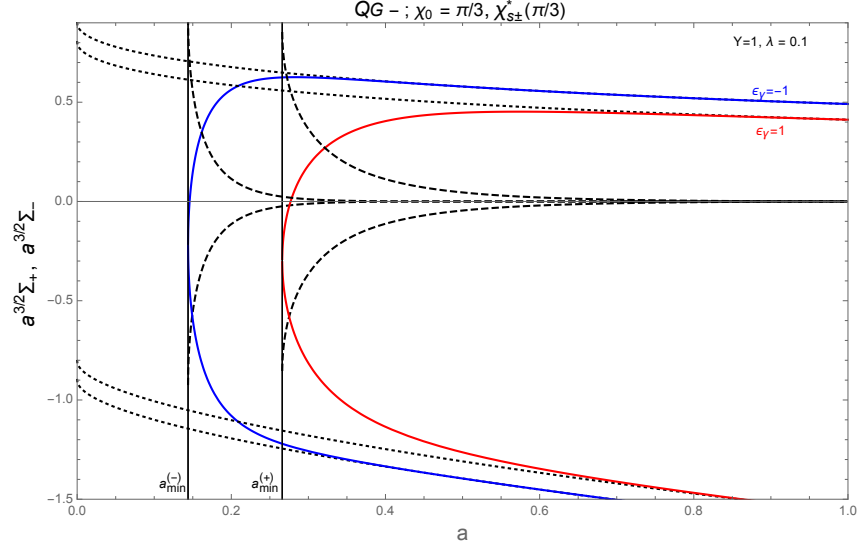


Figure 4. The evolution of $a^{3/2}\Sigma_+$ (positive) and $a^{3/2}\Sigma_-$ (negative) for a theory in which $\gamma = 1$ and $\lambda = 0.1$. The dotted lines correspond to the GR contribution, which is non-vanishing if the OS condition is not satisfied. The dashed line gives the extra-LQC contribution. The $\varepsilon = -1$ branch (blue line) is well-defined down to $a_{\min}^{(-)}$ and the $\varepsilon = +1$ branch (red line) down to $a_{\min}^{(+)}$. We chose $\chi_0 = \pi/3$ and the maximal allowed value of χ_s as given by Eq. (4.6).

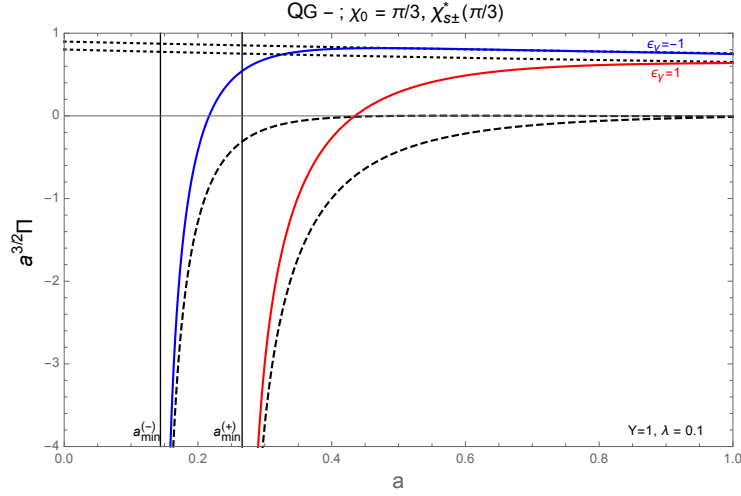


Figure 5. The evolution of $a^{3/2}\bar{\Pi}$ for a theory in which $\gamma = 1$ and $\lambda = 0.1$. The dotted lines correspond to the GR contribution, which is non-vanishing if the OS condition is not satisfied, the dashed line gives the extra-LQC contribution. The $\varepsilon = -1$ branch (blue line) is well-defined down to $a_{\min}^{(-)}$ and the $\varepsilon = +1$ branch (red line) down to $a_{\min}^{(+)}$. We chose $\chi_0 = \pi/3$ and the maximal allowed value of χ_s as given by Eq. (4.6).

at a radius above or at the Schwarzschild radius, the quantum corrections are not confined to the deep interior as usually assumed, but they are triggered at least at the horizon scale, or even on larger scales depending on the choice of the parameter λ . This provides a major

difference with current black-to-white hole bounce models recently discussed in the LQC literature, where quantum effects are dominant only near the Planck scale in the deep interior. However, a lesson of the present construction is that the scale at which the quantum effects become non-negligible shall not be set a priori, and consistency of the present model shows that they are actually relevant above and at the Schwarzschild radius.

While this might be an artefact due to the simplifying assumption of the model, this is nevertheless a major difference with current polymer constructions. Indeed, the recent polymer models of black hole interior assume from the beginning that quantum gravity effects are confined in the deep interior, which motivated the construction of modified μ_o -scheme regularization, see Refs.[38, 39] and more recently [42]. However, such choice is somehow not consistent with the standard improved dynamics used in the cosmological framework, and it would appear more natural to adopt the same strategy both for the loop regularization of cosmological and black hole backgrounds. In this regard, it is interesting to notice that once matter is coupled to gravity, the "pathological" features of the improved dynamics found in vacuum Kantowski-Sachs model disappear, as shown in Ref. [57]. From this point of view, it might be crucial to go beyond the case of vacuum bounce and include the role of collapsing matter to build consistent polymer models of bouncing compact object. Our model provides such a minimal construction using the standard LQC technics based on the $\bar{\mu}$ -scheme regularization.

4.2 Quantum vs classical collapse

4.2.1 The classical Oppenheimer-Snyder model with a thin shell

As discussed in the first section, the seminal OS model is constructed without assuming the presence of a thin-shell [78]. Hence, the present construction with $\Psi_1 = 0$ provides a classical extension of the initial OS model. Moreover, since $\Psi_1 = 0$ corresponds to the limit

$$\lambda = \frac{\tilde{\lambda}}{R_c} \rightarrow 0 \quad \Rightarrow \quad a_{\min}^{\pm} = 0 \quad (4.1)$$

this model actually corresponds to the classical limit of our Planck star construction for which $a \in [0, 1]$ such that the star can form a singularity. Notice that the classical limit, at fixed λ , corresponds to send the free parameter R_c to larger value, and thus to consider compact objects with lower and lower density, as expected.

Let us first discuss the reduced mass relation. Working in the classical framework with $\Psi_1 = 0$, it follows that the determinant (2.34) is positive only if

$$\sin \chi_s \leq \sin^3 \chi_0. \quad (4.2)$$

This provides a generalization of the seminal OS model, which corresponds to the case where the inequality is saturated. Solving the energy and pressure profiles of the thin shell in this generalized classical OS model, one finds there are two roots for Σ and the only non-negative one is given by

$$\Sigma_+ = \frac{1}{a} \left[\sqrt{\cot^2 \chi_0 + \left(\frac{\sin \chi_s}{\sin^3 \chi_0} - 1 \right) / a - \cot \chi_0} \right], \quad (4.3)$$

which diverges at the singularity $a = 0$, as expected. For that branch, the pressure is given by

$$\bar{\Pi} = -\frac{1}{a^2} \frac{\left(\frac{\sin \chi_s}{\sin^3 \chi_0} - 1 \right)}{\sqrt{\cot^2 \chi_0 + \left(\frac{\sin \chi_s}{\sin^3 \chi_0} - 1 \right) / a}}. \quad (4.4)$$

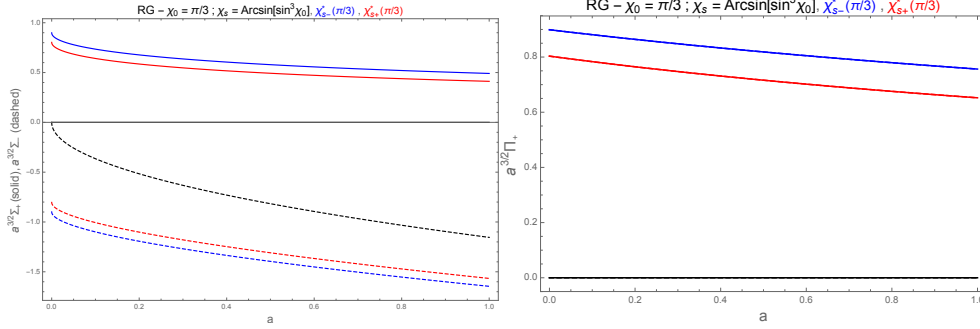


Figure 6. (Left) Evolution of $a^{3/2}\Sigma_+$ (positive) and $a^{3/2}\Sigma_-$ (non physical negative) in GR (i.e. assuming $\Psi_1 = 0$). When the OS condition holds then $\Sigma_+ = 0$. $\chi_{s\pm}^*$ is defined by Eq. (4.6) and those two curves shall be compared to Fig. 4. (Right) Evolution of Π .

Let us distinguish two cases. When (4.2) reduces to an equality, the model corresponds to the seminal derivation with the standard mass matching condition, where the junction condition are satisfied with $\Sigma = 0$. Indeed, in the case of equality, the determinant remains constant, and there is only one non-negative root, namely $\Sigma_+ = 0$. This corresponds to the most massive star, given χ_0 that can be described within the formalism.

Otherwise, when the star is less massive, the energy Σ of the thin shell enjoys two branches, one with negative energy that we shall regard as non-physical. The evolution of Σ with a is depicted on Fig. 6-left. Interestingly, the total energy of the shell, that scales as $\Sigma_+ a^2$ remains bounded for $a \in [0, 1]$. The surface pressure behaves as $a^{-3/2}$ so that $\bar{\Pi} a^2$ also remains bounded for $a \in [0, 1]$ and positive as long as the condition (4.2) holds. Its behavior is plotted in Fig. 6-right. Finally, it can also be checked that the equation of state of the shell is well approximated by

$$\Sigma_+ = \bar{\Pi},$$

which is exact in the limit $a \rightarrow 0$. This model corresponds to the classical limit of our Planck star.

4.2.2 Comparison of the dynamics and classical limit

As a last check, it is crucial to show that the modified dynamics matches with the classical relativistic dynamics when quantum effects become negligible, namely far away from the bounce. As one can see from Fig. 7, this is indeed the case. It confirms that our model has the correct classical limit far from the bounce and matches properly with the GR dynamics. Hence, the quantum corrections dominate only close to the bounce.

The two dynamics can also be compared in the phase space (a, \dot{a}) depicted on Fig. 8. It clearly shows that the OS trajectory for the collapsing star (and is symmetric describing an expanding star) defines a boundary in phase space in which the cycles of bounces allowed by

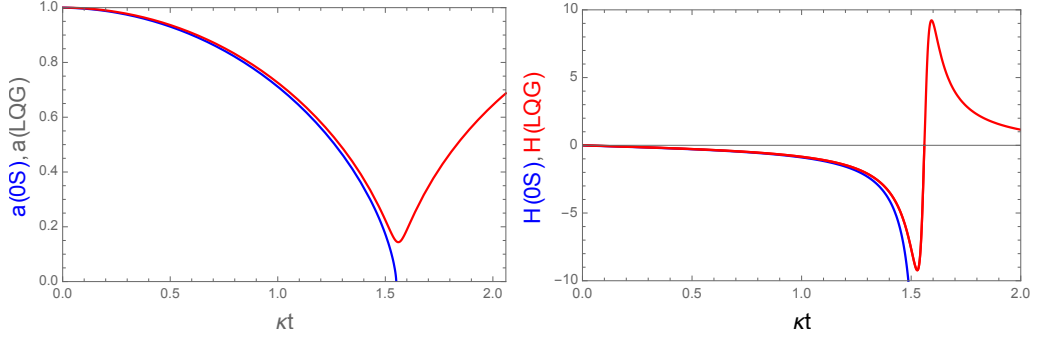


Figure 7. Comparison of the quantum induced bounce and the RG dynamics: (Left) Evolution of the scale factor for our Planck star (red) versus the classical GR collapse with thin shell (blue). (Right) Evolution of the Hubble rate for the Planck star (red) versus the classical GR collapse with a thin shell (blue).

quantum corrections are enclosed. It clearly shows how these corrections allow the dynamics to shift from the collapsing branch to the expanding branch.

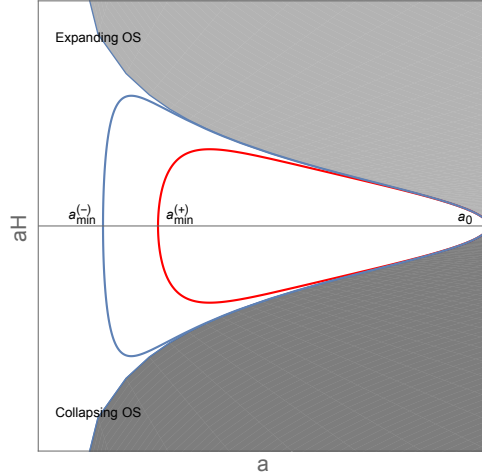


Figure 8. Dynamics of the collapsing OS star (black) compared to its quantum version, which exhibits cycle of two bounces (red and blue).

4.3 Phase diagram of the Planck star

Let us begin by discussing the phase diagram of our Planck star. The expression (2.35) of the surface energy Σ shows that it diverges when $a \rightarrow 0$. This implies that we have to impose that Δ remains positive. Such a condition sets constraints on the allowed range of parameters which satisfy the consistency condition of our model.

Since a is always larger than $a_{\min}^{(-)}$, Σ is well-defined if $\Delta(a_{\min}^{(-)}) \geq 0$. Keeping in mind that $\Psi_1(a_{\min}^{(-)}) = 1$, this condition rewrites as

$$a_{\min}^{(-)}(\lambda, \gamma) \geq \frac{\sin \chi_s}{\sin \chi_0}. \quad (4.5)$$

Since the parameters (λ, γ) are expected to be universal, and hence fixed once and for all, the above constraint implies that only a range of stars (χ_s, χ_0) can be described. This is summarized by Fig. 9. Hence, it is convenient to define

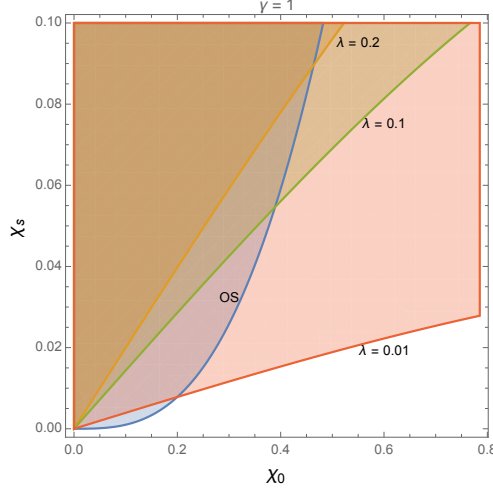


Figure 9. (Left) The range of stars that can be described by this formalism depends on the value of λ . The blue line corresponds to the OS condition. Below this curve, stars in GR can be described at the expense of introducing a shell.

$$\chi_{s\pm}^*(\lambda, \gamma) \equiv \arcsin \left[a_{\min}^{(\pm)}(\lambda, \gamma) \sin \chi_0 \right], \quad (4.6)$$

which, for any set of parameters (λ, γ) , gives the upper bound on χ_s that makes both bounces well-defined.

4.4 Orders of magnitude

Let us now discuss the order of magnitude of such a Planck star. The compact object described by our model is parametrized by five free parameters: $(\rho_{\min}, R_{\max}, M)$ which correspond to the physical parameters of the star, respectively to its initial density, its maximal radius and its mass together with the parameters of the theory, i.e. $(\tilde{\lambda}, \gamma)$ which encode the UV cut-off of the quantum theory and a freedom in defining the Ashtekar's variables. The BI parameter γ is mostly irrelevant and of order unity. The four remaining parameters need to satisfy

$$R_s \leq \left(\frac{\gamma \tilde{\lambda}}{R_c} \right)^{2/3} R_{\max} \quad \text{and} \quad \tilde{\lambda} < R_s < R_{\max} < R_c \quad (4.7)$$

The first condition is indeed the constraint (4.5) in which we used the fact that for small λ , $a_{\min} \sim \gamma^{2/3} \lambda^{2/3}$. The first inequality of the second condition is added to impose to ensure that the physical description is valid. Moreover, in order for our effective description to remain valid, the mass of the compact object has to be well above the Planck mass, i.e. $M/M_{\text{Planck}} \gg 1$.

In order to capture the domain of applicability imposed by the above consistency conditions, it is useful to introduce the quantity ξ defined by

$$\xi^2 \equiv \frac{4\pi}{3} \rho_{\min} \frac{R_{\max}^3}{M}, \quad (4.8)$$

so that a star without shell in GR will have $\xi = 1$. It follows that

$$R_c = \xi \frac{R_{\max}^{3/2}}{R_s^{1/2}}.$$

Hence, Eq. (4.7) rewrites as

$$R_s \leq \frac{\gamma \tilde{\lambda}}{\xi} \quad \text{and} \quad \tilde{\lambda} < R_s < R_{\max} < \xi \frac{R_{\max}^{3/2}}{R_s^{1/2}}. \quad (4.9)$$

We first conclude that independently of the radius of the star, its mass is constrained to be in the range

$$\tilde{\lambda} \leq R_s \leq \frac{\gamma \tilde{\lambda}}{\xi}, \quad (4.10)$$

from which we conclude that necessarily one need $\xi < 1$. Then the second set of constraints reduces to the boundary $R_s > \tilde{\lambda}$, $R_{\max} > R_s/\xi$ and $R_{\max} > R_s$, which is irrelevant when $\xi < 1$! The space of allowed models is summarized on Fig. 10. Note that $\tilde{\lambda}$ fixes all the scales of the problem and Eq. (4.10) implies that the mass of the star we want to describe set strong bounds on ξ if we want to have $\tilde{\lambda} \sim \mathcal{O}(\ell_P)$ and that its minimum radius is larger than $(\gamma/\xi)^{2/3} \tilde{\lambda}$ and the maximum density inside the star is smaller than $\rho_{\min}(\xi/\gamma)^2 (R_{\max}/\tilde{\lambda})^3$. Introducing $\hat{\lambda} \equiv \tilde{\lambda}/\ell_P$ we have

$$\hat{\lambda} \leq 1.8 \times 10^{38} \frac{M}{M_{\odot}} \leq \frac{\hat{\lambda}}{\xi},$$

where we have set $\gamma = 1$. Note that this implies that

$$\sin \chi_s = \frac{1}{\xi} \left(\frac{R_s}{R_{\max}} \right)^{3/2}, \quad \sin \chi_0 = \frac{1}{\xi} \left(\frac{R_s}{R_{\max}} \right)^{1/2},$$

so that $\sin \chi_s = \xi^2 \sin^3 \chi_0$.

Let us take two examples. First consider a Planck relic with $M = 10^{12} \text{kg}$ and $R_{\max} \simeq 10^{-14} \text{m}$ which mimics the order of magnitude considered initially in Ref. [1]. It shall satisfy $\hat{\lambda} \leq 10^{20} \leq \hat{\lambda}/\xi$ so that ξ has to be smaller than 10^{-20} and the smallest star that can be described is about $R_{\max} \sim 10^{20} \ell_P \sim 10^{-15} \text{m}$. Now, if one assumes $M = 1 \text{kg}$ then $\hat{\lambda} \leq 10^8 \leq \hat{\lambda}/\xi$ so that $\xi > 10^{-8}$ and one can have $R_{\max} \sim 10^8 \ell_P$. For Stellar mass objects then $M/M_{\odot} \sim 1$ so that one would need $\xi < 10^{-38}$. While mathematically possible, this will lead to stars with a density 10^{-38} smaller than the Solar density, hence smaller than 10^{-35}kg/m^3 , which is indeed unrealistic.

These orders of magnitude show that one can easily set $\tilde{\lambda}$ of the order of the Planck scale and describe relic black holes with the present model, but stellar massive compact objects cannot be modeled in a realistic manner within this construction. In turn, this restriction on the range of applicability of the model ensures that while the bounce takes place above or at the Schwarzschild radius, it still occurs in a high curvature regime as these planckian relics exhibit already very high curvature at the horizon scale. Finally, notice that within the range of masses discussed in the above examples, the planckian relics satisfy the conditions $M/M_{\text{Planck}} \gg 1$, which ensures the validity of the effective equations even for such extremely small mass and small size objects. See Ref. [81] for a discussion on this point.

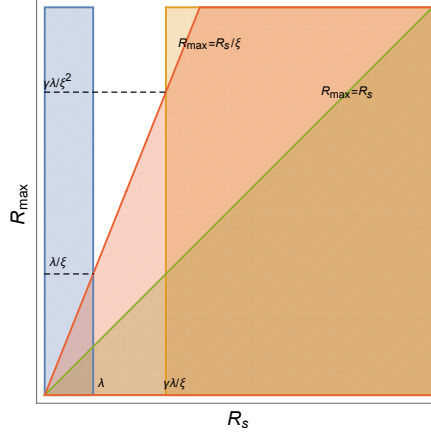


Figure 10. The parameter space of stars (R_s, R_{\max}) that are allowed given the parameters of the theory $(\tilde{\lambda}, \xi)$. Note that $\tilde{\lambda}$ fixes all the scale of the model.

5 Conclusion

Building on the effective construction presented in our companion article [65], this work has presented a new physical model for a bouncing compact object based on a quantum extension of the seminal OS model. This simple model of gravitational collapse, based on the thin-shell formalism, turns out to provide an ideal framework to bridge bouncing cosmological models to the description of bouncing compact objects. Let us summarize its main ingredients and its major outcomes.

First, the singularity resolution inside the interior of the star is obtained by replacing the classical closed FL universe by its LQC version based on the connection regularization [76, 77]. This loop regularization provides a concrete proposal for how the would-be singularity is replaced by a singularity free effective quantum geometry.

Then, our construction includes the matter sector. This allows us to go beyond current polymers approaches which largely focus solely on the vacuum spherically symmetric gravity phase space to discuss effective black-to-white hole bounce³. Moreover, our model provides also an alternative to matter collapse compared to the firework model, where matter is encoded in self-gravitating null shell. In our construction, even if highly idealized, the dust field provides a simpler and more physical matter content, and allows one to work with a time-like thin shell. This difference is crucial and is at the heart of our no-go result on the formation of trapped region. Indeed, with a null shell, one would not derived the expression (2.38) for the lapse at the surface of the star,. This explains the radical difference between our conclusions and those of the firework model.

The time-like thin-shell is crucial for the internal consistency of our approach. Indeed, it encodes part of the quantum effects and leads to a generalized version of the OS mass relation. The key constraint, given by Eq. (2.32), ensures the consistent matching of the conserved quantities of the exterior and interior geometries. From the general solution of the junction conditions presented in Ref. [65], we have discussed the behavior of the energy and pressure profile of the thin shell associated to a LQC bouncing interior geometry. As

³See however Ref. [57] for a study including matter in the Kawtowski-Sachs model and Refs. [58, 60–62] for few investigations regarding covariant matter plus gravity systems in inhomogeneous polymers models.

expected, quantum corrections become large near the bounce, and vanish far away for it. The classical limit of the model, which consists in the OS model with a non-vanishing thin shell, is well approximated at large radius.

The surprising outcome of our construction is that replacing the singular classical interior geometry with a bouncing geometry prevents from forming a trapped region. Hence, in such a UV complete gravitational collapse model, there is no formation of black hole. This provides a major deviation from the classical OS description of the collapse. We emphasize that this conclusion descends from i) demanding the continuity of the induced metric across the time-like thin shell and ii) modeling the exterior geometry with the Schwarzschild geometry which exhibits a single horizon. Relaxing this assumption and using an exterior geometry with an outer and inner horizon would allow the collapsing matter to form a trapped region and bounce inside the inner horizon. The present construction suggests therefore that the formation of an inner horizon is needed to build consistent black-to-white hole models based on matter collapse in which quantum gravity effects remain confined to the deep interior, in a high curvature regime.

Let us now summarize the phenomenology of our model. Since, the interior geometry enjoys both a UV cut-off, i.e $\tilde{\lambda}$ descending from the loop regularization, and an IR-cut-off R_c which encodes the energy density of the star prior to collapse. The compact object follows therefore cycles of collapse and expansion, with two consecutive distinct bounces. A novelty of the present construction is that the IR cut-off R_c is now a free parameter of the model, contrary to the classical OS model where it is fixed by once the mass and maximal radius are chosen, i.e once (χ_s, χ_0) are fixed. This freedom allows to explore new compact objects, which are much denser than the one described in GR, although not forming black holes. As it turns out, the energy scale at which quantum gravity become non-negligible is encoded in the ratio $\tilde{\lambda}/R_c$. Hence, at fixed $\tilde{\lambda}$, shifting the minimal energy of the compact object encoded in R_c allows to shift the scale at which quantum gravity becomes dominant. Finally, we have shown that the no-go result associated to this model, which translates into the constraint (4.7) onto the parameters, implies that this construction can be applied only to compact objects like Planckian relics but not to standard macroscopic stellar objects. This restriction of the range of applicability reconciles the no-go result presented in our companion paper [65] with the expectation that a quantum bounce, as the one considered here, shall occur only in a high curvature regime. Moreover, it is worth pointing that one can exhibit examples of such Planckian relics which satisfy the condition $M/M_{\text{Planck}} \gg 1$ such that the effective equations used in the present construction are still valid. This shows that, despite the rather surprising no-go result imposing the bounce above or at the Schwarzschild radius, the present highly idealized model can still be used to consistently model some range of planckian relics.

In conclusion, this model provides a mathematically consistent model of bouncing compact object within the LQC framework which realizes several crucial ideas introduced in the initial Planck star model in Ref. [1]. This construction should serve as a minimal set-up for further explorations regarding the modelization of bouncing compact objects using LQC technics. In particular, it would be interesting to compute the characteristic time of bounce associated to such Planckian relics and discuss its scaling w.r.t. the mass of the object. Additionally, it would be interesting to investigate the stability of such object, as an initial inhomogeneity would grow during the oscillation and the compact object would most probably follow only a finite number of cycles before being out of the range of validity of the present model. Finally, several simplifying assumptions of the present construction might be easily generalized to consider black-to-white hole bounce for macroscopic stellar objects,

such as introducing an inner horizon structure in the exterior geometry. We shall present some results in this direction in future works [82].

Acknowledgements

The work of JBA was supported by Japan Society for the Promotion of Science Grants-in-Aid for Scientific Research No. 17H02890. The authors thank Norbert Bodendorfer and Edward Wilson-Ewing for helpful suggestions on a previous version of this draft.

References

- [1] C. Rovelli and F. Vidotto, “Planck stars,” *Int. J. Mod. Phys. D* **23** (2014), no. 12, 1442026, [arXiv:1401.6562](#).
- [2] A. Ashtekar and P. Singh, “Loop Quantum Cosmology: A Status Report,” *Class. Quant. Grav.* **28** (2011) 213001, [arXiv:1108.0893](#).
- [3] A. Barrau and C. Rovelli, “Planck star phenomenology,” *Phys. Lett. B* **739** (2014) 405–409, [arXiv:1404.5821](#).
- [4] A. Barrau, B. Bolliet, F. Vidotto, and C. Weimer, “Phenomenology of bouncing black holes in quantum gravity: a closer look,” *JCAP* **1602** (2016), no. 02, 022, [arXiv:1507.05424](#).
- [5] A. Barrau, B. Bolliet, M. Schutten, and F. Vidotto, “Bouncing black holes in quantum gravity and the Fermi gamma-ray excess,” *Phys. Lett. B* **772** (2017) 58–62, [arXiv:1606.08031](#).
- [6] C. Rovelli, “Planck stars as observational probes of quantum gravity,” *Nat. Astron.* **1** (2017) 0065, [arXiv:1708.01789](#).
- [7] A. Barrau, F. Moulin, and K. Martineau, “Fast radio bursts and the stochastic lifetime of black holes in quantum gravity,” *Phys. Rev. D* **97** (2018), no. 6, 066019, [arXiv:1801.03841](#).
- [8] H. M. Haggard and C. Rovelli, “Quantum-gravity effects outside the horizon spark black to white hole tunneling,” *Phys. Rev. D* **92** (2015), no. 10, 104020, [arXiv:1407.0989](#).
- [9] T. De Lorenzo and A. Perez, “Improved Black Hole Fireworks: Asymmetric Black-Hole-to-White-Hole Tunneling Scenario,” *Phys. Rev. D* **93** (2016), no. 12, 124018, [arXiv:1512.04566](#).
- [10] S. Brahma and D. h. Yeom, “Effective black-to-white hole bounces: The cost of surgery,” *Class. Quant. Grav.* **35**, no. 20, 205007 (2018) [arXiv:1804.02821](#).
- [11] C. Rovelli and P. Martin-Dussaud, “Interior metric and ray-tracing map in the firework black-to-white hole transition,” *Class. Quant. Grav.* **35** (2018), no. 14, 147002, [arXiv:1803.06330](#).
- [12] F. D’Ambrosio and C. Rovelli, “How information crosses Schwarzschild’s central singularity,” *Class. Quant. Grav.* **35**, no. 21, 215010 (2018) [arXiv:1803.05015](#).
- [13] C. Barcelo, R. Carballo-Rubio, L. J. Garay, and G. Jannes, “The lifetime problem of evaporating black holes: mutiny or resignation,” *Class. Quant. Grav.* **32** (2015), no. 3, 035012, [arXiv:1409.1501](#).
- [14] C. Barcelo, R. Carballo-Rubio, and L. J. Garay, “Black holes turn white fast, otherwise stay black: no half measures,” *JHEP* **01** (2016) 157, [arXiv:1511.00633](#).
- [15] C. Barcelo, R. Carballo-Rubio, and L. J. Garay, “Exponential fading to white of black holes in quantum gravity,” *Class. Quant. Grav.* **34** (2017), no. 10, 105007, [arXiv:1607.03480](#).

- [16] E. Bianchi, M. Christodoulou, F. D’Ambrosio, H. M. Haggard, and C. Rovelli, “White Holes as Remnants: A Surprising Scenario for the End of a Black Hole,” *Class. Quant. Grav.* **35** (2018), no. 22, 225003, [arXiv:1802.04264](#).
- [17] C. Rovelli and F. Vidotto, “Pre-Big-Bang Black-Hole Remnants and Past Low Entropy,” *Universe* **4**, no. 11, 129 (2018) [arXiv:1805.03224](#).
- [18] C. Rovelli and F. Vidotto, “Small black/white hole stability and dark matter,” *Universe* **4**, no. 11, 127 (2018) [arXiv:1805.03872](#).
- [19] P. Martin-Dussaud and C. Rovelli, “Evaporating black-to-white hole,” *Class. Quant. Grav.* **36**, no. 24, 245002 (2019) [arXiv:1905.07251](#).
- [20] H. Kawai, Y. Matsuo and Y. Yokokura, “A Self-consistent Model of the Black Hole Evaporation,” *Int. J. Mod. Phys. A* **28**, 1350050 (2013) [arXiv:1302.4733](#).
- [21] V. Baccetti, S. Murk and D. R. Terno, “Black hole evaporation and semiclassical thin shell collapse,” *Phys. Rev. D* **100**, no. 6, 064054 (2019) [arXiv:1812.07727](#).
- [22] P. M. Ho, H. Kawai, Y. Matsuo and Y. Yokokura, “Back Reaction of 4D Conformal Fields on Static Geometry,” *JHEP* **1811**, 056 (2018) [arXiv:1807.11352](#).
- [23] P. M. Ho, Y. Matsuo and Y. Yokokura, “An Analytic Description of Semi-Classical Black-Hole Geometry,” [arXiv:1912.12855](#).
- [24] S. V. Bolokhov, K. A. Bronnikov and M. V. Skvortsova, “The Schwarzschild singularity: a semiclassical bounce?,” *Grav. Cosmol.* **24**, no. 4, 315 (2018) [arXiv:1808.03717](#).
- [25] A. Ashtekar and M. Bojowald, “Quantum geometry and the Schwarzschild singularity,” *Class. Quant. Grav.* **23** (2006) 391–411, [arXiv:gr-qc/0509075](#).
- [26] L. Modesto, “Black hole interior from loop quantum gravity,” *Adv. High Energy Phys.* **2008** (2008) 459290, [arXiv:gr-qc/0611043](#).
- [27] C. G. Boehmer and K. Vandersloot, “Loop Quantum Dynamics of the Schwarzschild Interior,” *Phys. Rev. D* **76** (2007) 104030, [arXiv:0709.2129](#).
- [28] C. G. Boehmer and K. Vandersloot, “Stability of the Schwarzschild Interior in Loop Quantum Gravity,” *Phys. Rev. D* **78** (2008) 067501, [arXiv:0807.3042](#).
- [29] L. Modesto and I. Premont-Schwarz, “Self-dual Black Holes in LQG: Theory and Phenomenology,” *Phys. Rev. D* **80** (2009) 064041, [arXiv:0905.3170](#).
- [30] D.-W. Chiou, W.-T. Ni, and A. Tang, “Loop quantization of spherically symmetric midisuperspaces and loop quantum geometry of the maximally extended Schwarzschild spacetime,” [arXiv:1212.1265](#).
- [31] R. Tibrewala, “Spherically symmetric Einstein-Maxwell theory and loop quantum gravity corrections,” *Class. Quant. Grav.* **29**, 235012 (2012) [arXiv:1207.2585](#).
- [32] R. Gambini and J. Pullin, “Loop quantization of the Schwarzschild black hole,” *Phys. Rev. Lett.* **110**, no. 21, 211301 (2013) [arXiv:1302.5265](#).
- [33] A. Corichi and P. Singh, “Loop quantization of the Schwarzschild interior revisited,” *Class. Quant. Grav.* **33**, no. 5, 055006 (2016) [arXiv:1506.08015](#).
- [34] J. Olmedo, S. Saini and P. Singh, “From black holes to white holes: a quantum gravitational, symmetric bounce,” *Class. Quant. Grav.* **34**, no. 22, 225011 (2017) [arXiv:1707.07333](#).
- [35] J. Cortez, W. Cuervo, H. A. Morales-Tıcoltı and J. C. Ruelas, “Effective loop quantum geometry of Schwarzschild interior,” *Phys. Rev. D* **95**, no. 6, 064041 (2017) [arXiv:1704.03362](#).
- [36] J. Ben Achour, F. Lamy, H. Liu and K. Noui, “Polymer Schwarzschild black hole: An effective metric,” *EPL* **123**, no. 2, 20006 (2018) [arXiv:1803.01152](#).

- [37] M. Bojowald, S. Brahma and D. h. Yeom, “Effective line elements and black-hole models in canonical loop quantum gravity,” *Phys. Rev. D* **98**, no. 4, 046015 (2018) [arXiv:1803.01119](#).
- [38] A. Ashtekar, J. Olmedo and P. Singh, “Quantum extension of the Kruskal spacetime,” *Phys. Rev. D* **98**, no. 12, 126003 (2018) [arXiv:1806.02406](#).
- [39] N. Bodendorfer, F. M. Mele and J. M  ijnc, “A note on the Hamiltonian as a polymerisation parameter,” *Class. Quant. Grav.* **36**, no. 18, 187001 (2019) [arXiv:1902.04032](#).
- [40] M. Bojowald, “Comment (2) on "Quantum Transfiguration of Kruskal Black Holes",” [arXiv:1906.04650](#).
- [41] M. Bouhmadi-Lopez, S. Brahma, C. Y. Chen, P. Chen and D. h. Yeom, “Comment on "Quantum Transfiguration of Kruskal Black Holes",” [arXiv:1902.07874](#).
- [42] N. Bodendorfer, F. M. Mele and J. M  ijnc, “Effective Quantum Extended Spacetime of Polymer Schwarzschild Black Hole,” *Class. Quant. Grav.* **36**, no. 19, 195015 (2019) [arXiv:1902.04542](#).
- [43] N. Bodendorfer, F. M. Mele and J. M  ijnc, “(b,v)-type variables for black to white hole transitions in effective loop quantum gravity,” [arXiv:1911.12646](#).
- [44] N. Bodendorfer, F. M. Mele and J. M  ijnc, “Mass and Horizon Dirac Observables in Effective Models of Quantum Black-to-White Hole Transition,” [arXiv:1912.00774](#).
- [45] M. Bojowald, S. Brahma and J. D. Reyes, “Covariance in models of loop quantum gravity: Spherical symmetry,” *Phys. Rev. D* **92**, no. 4, 045043 (2015) [arXiv:1507.00329](#).
- [46] D. Aruga, J. Ben Achour and K. Noui, “Deformed General Relativity and Quantum Black Holes Interior,” [arXiv:1912.02459](#).
- [47] J. Ben Achour, F. Lamy, H. Liu and K. Noui, “Non-singular black holes and the Limiting Curvature Mechanism: A Hamiltonian perspective,” *JCAP* **1805**, 072 (2018) [arXiv:1712.03876](#).
- [48] M. Assanioussi, A. Dapor and K. Liegener, “Perspectives on the dynamics in a loop quantum gravity effective description of black hole interiors,” [arXiv:1908.05756](#).
- [49] E. Alesci, S. Bahrami and D. Pranzetti, “Quantum evolution of black hole initial data sets: Foundations,” *Phys. Rev. D* **98**, no. 4, 046014 (2018) [arXiv:1807.07602](#).
- [50] E. Alesci, S. Bahrami and D. Pranzetti, “Quantum gravity predictions for black hole interior geometry,” *Phys. Lett. B* **797**, 134908 (2019) [arXiv:1904.12412](#).
- [51] M. Bojowald, R. Goswami, R. Maartens, and P. Singh, “A Black hole mass threshold from non-singular quantum gravitational collapse,” *Phys. Rev. Lett.* **95** (2005) 091302, [arXiv:gr-qc/0503041](#).
- [52] Y. Tavakoli, J. Marto, and A. Dapor, “Dynamics of apparent horizons in quantum gravitational collapse,” *Springer Proc. Math. Stat.* **60** (2014) 427–431, [arXiv:1306.3458](#).
- [53] Y. Tavakoli, J. Marto, and A. Dapor, “Semiclassical dynamics of horizons in spherically symmetric collapse,” *Int. J. Mod. Phys. D* **23** (2014), no. 7, 1450061, [arXiv:1303.6157](#).
- [54] C. Bambi, D. Malafarina, and L. Modesto, “Non-singular quantum-inspired gravitational collapse,” *Phys. Rev. D* **88** (2013) 044009, [arXiv:1305.4790](#).
- [55] Y. Liu, D. Malafarina, L. Modesto, and C. Bambi, “Singularity avoidance in quantum-inspired inhomogeneous dust collapse,” *Phys. Rev. D* **90** (2014), no. 4, 044040, [arXiv:1405.7249](#).
- [56] S. Campbell, “Models of Non-Singular Gravitational collapse,” Ph.D Thesis **London SW7 2AZ** (2014).

- [57] A. Joe and P. Singh, “Kantowski-Sachs spacetime in loop quantum cosmology: bounds on expansion and shear scalars and the viability of quantization prescriptions,” *Class. Quant. Grav.* **32**, no. 1, 015009 (2015) [arXiv:1407.2428](#)
- [58] R. Gambini and J. Pullin, “Quantum shells in a quantum space-time,” *Class. Quant. Grav.* **32**, no. 3, 035003 (2015) [arXiv:1408.4635](#)
- [59] J. Ziprick, J. Gegenberg and G. Kunstatter, “Polymer Quantization of a Self-Gravitating Thin Shell,” *Phys. Rev. D* **94**, no. 10, 104076 (2016) [arXiv:1609.06665](#)
- [60] J. Ben Achour, S. Brahma and A. Marciano, “Spherically symmetric sector of self dual Ashtekar gravity coupled to matter: Anomaly-free algebra of constraints with holonomy corrections,” *Phys. Rev. D* **96**, no. 2, 026002 (2017) [arXiv:1608.07314](#)
- [61] J. Ben Achour and S. Brahma, “Covariance in self dual inhomogeneous models of effective quantum geometry: Spherical symmetry and Gowdy systems,” *Phys. Rev. D* **97**, no. 12, 126003 (2018) [arXiv:1712.03677](#)
- [62] M. Bojowald, S. Brahma, D. Ding and M. Ronco, “Deformed covariance in spherically symmetric vacuum models of loop quantum gravity: Consistency in Euclidean and self-dual gravity,” [arXiv:1910.10091](#)
- [63] R. Carballo-Rubio, F. Di Filippo, S. Liberati and M. Visser, “Opening the Pandora’s box at the core of black holes,” [arXiv:1908.03261](#).
- [64] R. Carballo-Rubio, F. Di Filippo, S. Liberati and M. Visser, “Geodesically complete black holes,” [arXiv:1911.11200](#).
- [65] J. Ben Achour, S. Brahma and J-P. Uzan, “Bouncing compact object I: Quantum extension of the Oppenheimer-Snyder model,” (2019)
- [66] T. De Lorenzo, C. Pacilio, C. Rovelli and S. Speziale, “On the Effective Metric of a Planck Star,” *Gen. Rel. Grav.* **47**, no. 4, 41 (2015) [arXiv:1412.6015](#).
- [67] C. Barcelo, R. Carballo-Rubio, and L. J. Garay, “Gravitational wave echoes from macroscopic quantum gravity effects,” *JHEP* **05** (2017) 054, [arXiv:1701.09156](#).
- [68] R. Carballo-Rubio, F. Di Filippo, S. Liberati, C. Pacilio, and M. Visser, “On the viability of regular black holes,” *JHEP* **07** (2018) 023, [arXiv:1805.02675](#).
- [69] R. Carballo-Rubio, F. Di Filippo, S. Liberati, and M. Visser, “Phenomenological aspects of black holes beyond general relativity,” *Phys. Rev. D* **98** (2018), no. 12, 124009, [arXiv:1809.08238](#).
- [70] R. Brandenberger and P. Peter, “Bouncing Cosmologies: Progress and Problems,” *Found. Phys.* **47** (2017), no. 6, 797–850, [arXiv:1603.05834](#).
- [71] D. Battefeld and P. Peter, “A Critical Review of Classical Bouncing Cosmologies,” *Phys. Rept.* **571** (2015) 1–66, [arXiv:1406.2790](#).
- [72] W. Israel, “Singular hypersurfaces and thin shells in general relativity,” *Nuovo Cim.* **B44S10** (1966) 1. [*Nuovo Cim.*B44,1(1966)].
- [73] C. Barrabes and W. Israel, “Thin shells in general relativity and cosmology: The Lightlike limit,” *Phys. Rev. D* **43** (1991) 1129–1142.
- [74] A. Ashtekar, T. Pawłowski, P. Singh and K. Vandersloot, “Loop quantum cosmology of $k=1$ FRW models,” *Phys. Rev. D* **75**, 024035 (2007) [arXiv:0612104](#).
- [75] L. Szulc, W. Kaminski and J. Lewandowski, “Closed FRW model in Loop Quantum Cosmology,” *Class. Quant. Grav.* **24**, 2621 (2007) [arXiv:0612101](#).
- [76] A. Corichi and A. Karami, “Loop quantum cosmology of $k=1$ FRW: A tale of two bounces,” *Phys. Rev. D* **84**, 044003 (2011) [arXiv:1105.3724](#).

- [77] J. L. Dupuy and P. Singh, “Implications of quantum ambiguities in $k=1$ loop quantum cosmology: distinct quantum turnarounds and the super-Planckian regime,” *Phys. Rev. D* **95**, no. 2, 023510 (2017) [arXiv:1608.07772](#).
- [78] J. R. Oppenheimer and H. Snyder, “On Continued gravitational contraction,” *Phys. Rev.* **56** (1939) 455–459.
- [79] A. Corichi and A. Karami, “Loop quantum cosmology of $k = 1$ FLRW: Effects of inverse volume corrections,” *Class. Quant. Grav.* **31**, 035008 (2014) [arXiv:1307.7189](#)
- [80] J. L. Dupuy and P. Singh, “Hysteresis and beats in loop quantum cosmology,” [arXiv:1912.11490](#)
- [81] C. Rovelli and E. Wilson-Ewing, “Why are the effective equations of loop quantum cosmology so accurate?,” *Phys. Rev. D* **90**, no. 2, 023538 (2014) [arXiv:1310.8654](#).
- [82] J. Ben Achour, S. Brahma, S. Mukohyama and J-P. Uzan, “to appear” (2020)